Vadim Kim and Afanasiy Ostrik

View Online   Export Citation

ARTICLES YOU MAY BE INTERESTED IN

Computer Modeling of the Effect of Aircraft Impact on the Containment of Nuclear Power Plant

Vadim Kim[a)] and Afanasiy Ostrik

Institute of Problems of Chemical Physics
Ac. Semenov Ave. 1, Chernogolovka, Moscow region, 142432 Russian Federation

[a)]Corresponding author: kim@ficp.ac.ru

Abstract. A new version of the governing equations for concrete is proposed. A numerical algorithm for solving the governing equations proposed has been developed. The developed algorithm is implemented as part of numerical 3D-code for the finite-size particle in cell method. Using the code the simulation of an airliner engine impact on the concrete containment was performed. It was obtained that engines with the speed of 100 m/s significantly damage the containment structure, but without full penetration (the engines stop right inside the protective shield). Nonetheless the total collapse of the central part of spherical dome onto the inner metal shell of the containment is probable when the engine impacts in downward direction.

INTRODUCTION

One of the possible sources of impact hazard for nuclear power plants (NPP) is falling aircraft [1-3]. The aircraft crashes are very rare but potentially extremely severe events. The probability of an accidental fall of a heavy airliner on a nuclear reactor is negligible: no more than 10-6 accidents per year [4]. In other words one aircraft crash can be realized within a million years if the plane airways are located near NPP. But the consequences of such an accident are catastrophic and cannot be ignored while designing NPP containments. Moreover, the location of NPP in the area of busy airway traffic is not exceptional and takes place for a number of nuclear power plants around the globe. As well as it is impossible to exclude the case of intended direction of the plane on the nuclear reactor in terrorist acts. Therefore the probability of aircraft crash for each NPP is estimated individually taking into account specific air traffic situation. If the value of probability is less than 10-6 per year, then the possibility of the accident is ignored [5]. Otherwise it is taken as considerable.

It is generally accepted to consider three types of aircrafts in this regard: General Aviation (GA - small aircrafts including private and sporting flight vehicles), Military Aviation (MA) and Commercial Air Transport (CAT). According to safety regulations the impact of GA-aircrafts is persistently taken into account when designing the NPP infrastructure. This norm is justified by high accident rate for such type of aircrafts. Accidents with Military and Commercial airplanes are considered in conjunction with the air traffic situation in the NPP area. Note that despite the lower mass MA-aircraft creates a larger load than CAT ones. According to the Riera formula [6] the dynamic load component is proportional to the square of the aircraft speed, which is significantly higher for military aircrafts. However hijacking act for MA aircraft is much less probable than for CAT planes, and considering the impact of large mainline aircrafts represents the great interest. Boeing 707-320 and Boeing 747-400 aircraft types are the most common and widespread among mainline aircrafts. For many countries Boeing 707-320 is the standard for a commercial aircraft when calculating an impact with NPP. Many works [3-5] are devoted to the modeling of impact action of these aircraft types on NPP containments.

As a rule the nuclear reactor containment is a double-wall construction. Typical external nutshell is made of concrete composition, inner barrier is a thin-walled metal shell. The external concrete wall is designed to protect the reactor from external mechanical and thermal loading (impacts, shock waves, high intensity radiation and particles

beams, etc.). The inner metal shell has multiple function, e.g. reactor zone isolation from spilled liquid fuel after the aircraft strikes the NPP (Boeing 707-320 can carry up to 75 tons of jet fuel).

The fuselage body of an aircraft is a low-strength object when compared to the NPP containment. It can be considered as a thin-shell construction interacting with massive concrete wall. Characteristic timescale for this process is ~10-1 seconds [6,7], which is much slower than for the disturbance (acoustic) wave propagation through the thickness of concrete wall. That is why when we consider the impact of delicate low-density aircraft fuselage body - the thin-shell stage of deformation of containment prevails. Note that while being low-strength, easily collapsible and highly deformable but very massive the aircraft fuselage body gives the containment a significant amount of momentum during the interaction (up to 20 MN×s for a Boeing 707-320), which can lead to collapse of the containment wall during the thin-shell stage of deformation process.

On the other hand aircraft engines have greater penetration ability. In the concentrated impact loading of containment wall by compact, dense and rigid engines the wave stage prevails. It is the engines impact mainly can lead to the penetration of the containment shell with the subsequent spilling of liquid fuel into the active core of the nuclear reactor.

Also should be noted that generally reinforced concrete is used for NPP constructions. Internal metal armoring allows to increase the load-carrying capacity of concrete and it is essential for thin-shell stage of NPP loading simulations. But as we consider the wave stage of the process of penetration, addition of internal armoring beams will weaken the shell overall: introduction of multiple internal contact surfaces between two materials with very different dynamic impedance (steel and concrete) will lead to complex shock-wave reverberation, formation of internal release rarefraction waves, splitting on contacts of materials and spall fracture in concrete. So the wave stage modeling for solid pure concrete wall is an upper bound estimate for the 'aircraft engine-NPP concrete shell' impact.

METHODS AND MODELS

In this work the values of aircraft velocity are limited by a reasonable limit of ~ 100 m/s (~ 360 km/h). Thus the impact have to be considered as a low-speed interaction (i.e. < 1 km/s) and elastic-plastic deformations and shear stresses are have to be included into consideration.

Dynamic impact loading of concrete leads to non-stationary hydrodynamic flow with high deformation rates, high pressures as well as birth, growth and accumulation of defects in brittle fractured material. As a result the system of macro cracks is formed. So adequate non-stationary models of concrete dynamic behavior are required.

Models of Non-Stationary Deformation and Fracture of Concrete

Dynamic impact loading of concrete leads to non-stationary hydrodynamic flow with high deformation rates, high pressures as well as birth, growth and accumulation of defects in brittle fractured material. As a result the system of macro cracks is formed. So adequate non-stationary models of concrete dynamic behavior are required.

High pressures during the process do not allow us to use simple linear models for deviatoric part of the stress tensor. Therefore nonlinear equation of the state of concrete is used combined with irreversible compaction of pores model. At the same time it is possible to neglect thermal part in the pressure equation for many practical applications with low-speed impacts.

Accumulation of material defects during the impact have to be taken into account, corresponding kinetic models with scalar (or vector) medium damage characteristic values have to be considered. The formulation of the system of damage kinetic equations is a complex and unresolved problem to this day. As the most primitive approach a linear model is used, where the increment of scalar damage value is directly proportional to the increment of total (volume and shear) plastic deformations with the proportionality coefficient depending on pressure.

Concrete is rate dependent material in terms of velocity of the loading. First of all the influence of strain rate on the yield surface configuration have to be considered: the yield surface grows with the increase of the deformation rate. Also the damage and pressure levels have a significant effect on the yield surface. It is common practice to simplify the simulation model the yield surface - strain rate dependence is separated as a standalone multiplier.

Thus the use of joint models of elastic-plastic flow and material fracture [8] and effects of viscosity is needed to adequately describe concrete materials behavior.

The phenomenon of birth-and-growth of the macro cracks system with a definite predominant direction makes the behavior of concrete as of a specifically anisotropic material. The need for description of anisotropic effects

emerging in the process of deformation complicates the simulations significantly. Another anisotropic feature of the concrete is a considerable difference in tensile and compression strengths.

A separate and very important problem is the quantitative definition of parameters for the numerical models for a specific concrete material. As a facilitation factor may be used that if there are definite physical meaning or parametric correlation relationship exist, both between different parameters and between the same parameter values for different concrete specimens (scale effects).

At the moment there is no universal model for adequate description of dynamic loading of concrete. We have to dissect and choose the model for specific physical detailing level needed, simulation accuracy required and available CPU-power. That is why a sufficient software product for simulation of dynamic loading of concrete objects in 3D should include multiple models of deformation and fracture of cement compositions: the Gineev concrete model, the Holmquist-Johnson-Cook model (HJC-model) [9], the Perzyna elastic-viscoplasticity model [10], the Gurson-Tvergaard-Needleman structural micromechanical model (GTN-model) [11-13], the Kukudzhanov structural two-level micromechanical model [14].

Only the first two of these models are provided with the constants for specific concrete compositions and can be used in our simulations of aircraft engines impact on concrete NPP containment shell. A numerical algorithm for realizing the governing equations of the HJC-model is described in [9]. This model is not sensitive to the third stress tensor invariant. G A Gineev's deformation theory of plasticity does not have this defect, but is applicable for static problems and for the basic loading trajectories only. Also this model does not include damages accumulation. It would be helpful to combine these two models.

For the generalization we describe the behavior of concrete as in the HJC-model except for the plastic yield surface, in which we apply synthetic approach (1):

$$\left(\frac{T_S}{T_C}\right)^2 = \left(1 - D + f\frac{P}{T_C}\right)\left(1 + C\ln(\dot{\varepsilon}_i)\right)^2 (1 + \delta),$$ 1

$$\delta = e\left(\frac{S(1 + C\ln(\dot{\varepsilon}_i))}{T_S}\right)^3, \quad f = \frac{3T_C(R_C - R_P)}{R_C R_P}, \quad e = \frac{R_C R_P}{3T_C^2} - 1,$$

$$T_S = \frac{1}{\sqrt{2}}\sqrt{S_{xx}^2 + S_{yy}^2 + S_{zz}^2 + 2\left(\sigma_{xy}^2 + \sigma_{xz}^2 + \sigma_{yz}^2\right)},$$

$$S^3 = \frac{\sqrt{3}}{2}\left(S_{xx}^2 + S_{yy}^2 + S_{zz}^2 - 3\left(\sigma_{xy}^2 S_{zz} + \sigma_{xz}^2 S_{yy} + \sigma_{yz}^2 S_{xx}\right) + 6\sigma_{xy}\sigma_{xz}\sigma_{yz}\right),$$ (1)

where P – pressure; T_s – limit intensity of tangential stresses (it's root of the second invariant of the deviator of stresses tensor); D – scalar damage value; S – an invariant (the cube of this value is proportional to the third invariant the deviator of stresses tensor); R_C, R_P, T_C – strength limits of concrete at uni-axial compression, stretching and pure shear; C, f, e – constants; $\dot{\varepsilon}_i$ – intensity of strain rates.

The correction $\delta = \delta(S)$ is included in (1) for the effect of third invariant S on the yield surface; the multiplier $1 + C\ln(\dot{\varepsilon}_i)$ is for influence of the strain rates as in the HJC-model. C - constant has the same meaning and value as in the HJC-model, which is helpful as it is defined for many concrete types.

The calculation of the damage value is made as in the HJC-model, where the increment of damage is proportional to the increment of total plastic deformation (2):

$$\Delta D = \frac{\Delta\varepsilon^p + \Delta\mu^p}{\max\left(\varepsilon_{f\min}, D_1\left(\frac{p}{R_C} + \frac{R_{pg}}{R_C}\right)^{D_2}\right)},$$ 2

$$\Delta\varepsilon^p = \Delta\varepsilon_i - \frac{\Delta T}{\sqrt{3}G}, \quad \Delta\mu^p = \Delta\left(\mu - \frac{P}{K(\mu)}\right),$$

where $\Delta\varepsilon^p$, $\Delta\mu^p$ – increments of shear and volume plastic deformations; D_1, D_2 – material parameters; $\varepsilon_{f\min}$ – parameter introduced to suppress the accumulation of damage from weak tensile waves; R_{pg} – limit strength at uniform stretching.

The proposed model of plastic deformation and fracture of concrete is fundamentally non-linear and have to be implemented using iterations. Iterations have to be performed in every calculation cell and hence have to converge quickly. In practice the accuracy required (relative error < 0.1%) is achieved in 3-5 iteration cycles. For the material parameters we use correlation relations.

If we define current stress state: $\sigma_{ij}^{n+1} = -P^{n+1}\delta_{ij} + S_{ij}^{n+1}$, ($i$=$x$,$y$,$z$; j=x,y,z; δ_{ij} – Kronecker delta) and damage degree D^{n+1} at t^{n+1}, then densities ρ^n, ρ^{n+1}, damage degree D^n, pressure P^n, tensor components S_{ij}^n, $\dot\varepsilon_{ij}^{n+\frac{1}{2}}$ are assumed to be known. The algorithm of this determination involves iterations by the damage degree D^{n+1} and the invariant value S^{n+1}. The calculation of the stress state on each iteration is based on the Wilkins approach [15]. Pressure P^{n+1} is calculated from the specified density and damage value in a separate subroutine-function: $P^{n+1} = F_{press}(P^n, \rho^n, \rho^{n+1}, D^{n+1})$, according to the HJC-model. This numerical algorithm is a further development of the algorithm considered in [9].

Finite-size Particles-in-cell Method for Gas Dynamics Simulation

For the hydrodynamic simulation of compressible flow in 3D we use finite-size particles-in-cell method [16] which is based on original particles-in-cell method [17].

It uses the Lagrangian–Eulerian representation of media which allows one to simulate flows with strong deformations. An ensemble of compressible finite-sized rectilinear Lagrangian particles moves through rectangular Eulerian grid that being used for definition of field parameters (pressure, stresses, mass velocity, etc.) and its derivatives. Defined finite size of the particles allows us to minimize amount of particles per cell needed for smooth results (no more than 1 particle/cell for every material). At the end of every time-step calculated the particles are regrouped by splitting/merging procedure to prevent artificial voids formation and any local irregularities in the particles system. Particle nature of the method allows to implement different physical/material models for multi-body multi-phase flows with complex internal contact surfaces and free surfaces tracking, body fragmentation, etc. Also the regular 'grid-particle' data model fits for massive parallel computing and widespread distributed memory cluster supercomputers can be utilized. Artificial viscous pressure in Von Neumann-Richtmyer form is used for calculating shocks.

Modern models of thermodynamic properties of matter, particle beams energy deposition, elastic-plastic deformation and fracture have been implemented in the hydro code adapted for parallel computations. This code was successfully used for 2D and 3D simulation of different High Energy Density physics phenomena: hypervelocity impact [16], high-pressure equation of state of matter experiments using high-explosives [18], intense heavy ion beam experiments [19,20], planetary science [21,22].

RESULTS OF NUMERICAL MODELING

The impact of one individual engine on the spherical dome of the concrete NPP containment shell was considered. Geometry and dimensions are shown on Fig. 1. For simplification the engine of the BOEING 707-320 was simulated as a compact iron ball of the same mass m = 2000 kg with a radius of 0.394 m and normal velocity V0 = 100 m/s.

Results of 3D computer modeling are shown on Figs. 2, 3 and 4. Axial cross sections of the damage value D (Fig. 2) and density (Fig. 3) are presented for different moments of time, as well as for 3D damage value D distribution (Fig. 4). One can see that fractured areas with D ≥ 1 in the dome (red zones on the Figs. 2 and 4) are located mainly near the free surfaces and in front of the impacting engine. The corresponding large cracks evolved in concrete (Fig. 3). The compacting zone is formed in concrete in front of the engine. This leads to engine's gradual slowdown and stop when the engine gets stuck in the concrete. But all the concrete material near the engine is fractured throughout the full thickness of the wall (~ 2 m cylindrical corridor at t = 4 ms). Then the total collapse of fractured fragment of the spherical dome down to the internal metal shell of the containment is very probable.
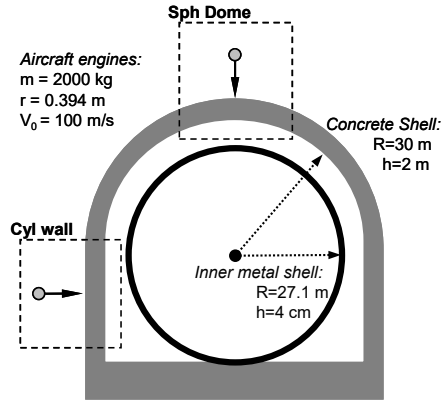
FIGURE 1. Schematic NPP-containment geometry and computational configurations for impact on spherical dome and cylindrical wall configurations
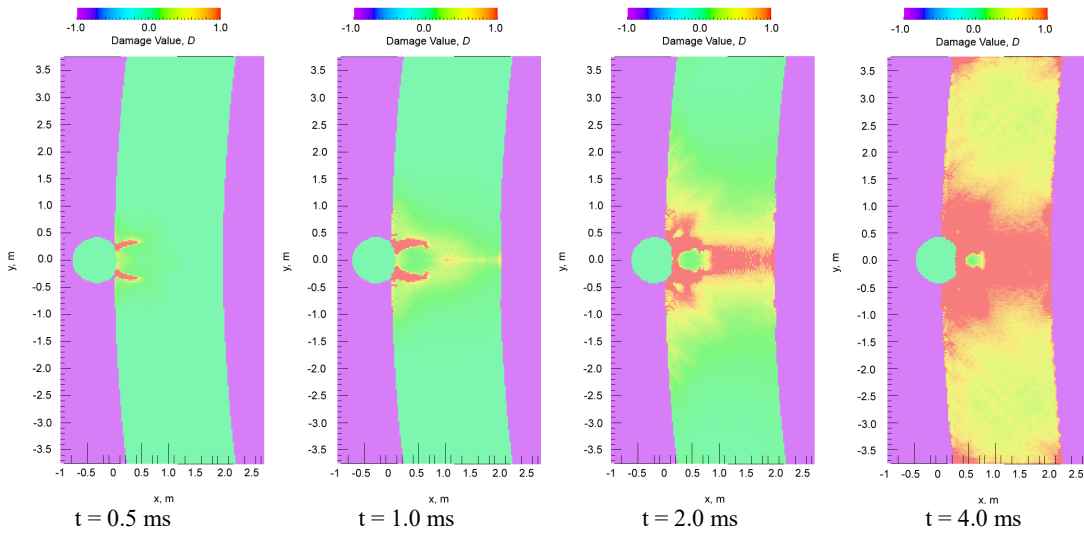
FIGURE 2. 2D-distribution of the damage value (*D*) in the spherical dome
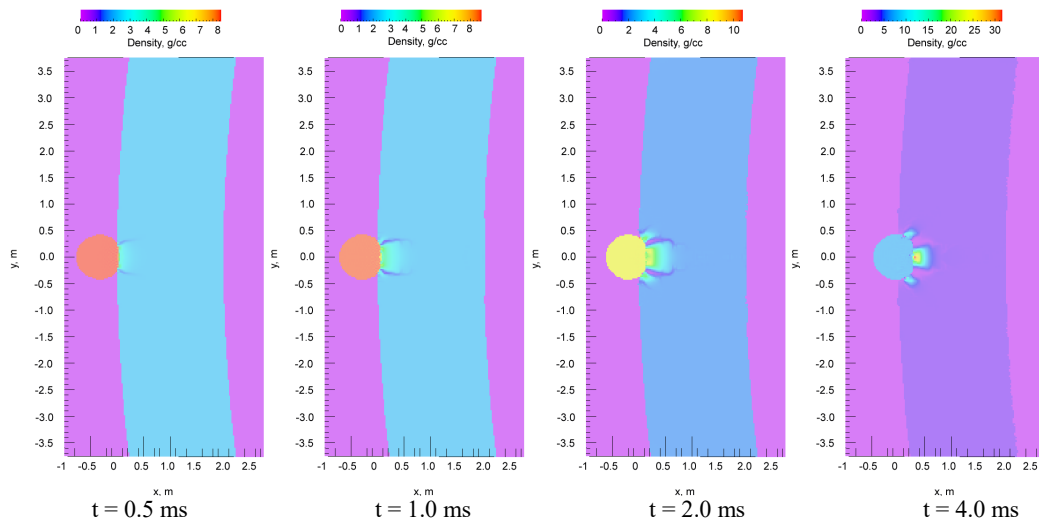
FIGURE 3. 2D-distribution of the density in the spherical dome and projectile

The BOEING 707-320 aircraft has four engines. In the condition of lateral side impact of an aircraft on the cylindrical part of containment wall - due to the curvature of the wall - the far pair of the engines start to interact with the containment much later compared to the timescale of the wave stage. That is why for the wave stage it is appropriate to consider the impact of two central engines separately.

Results of numerical simulation for distribution of damage value D in different moments of time are shown in Fig. 5. Position of the distant pair of engines is also presented for clarity. The red fracture zones and areas of compression in concrete are localized in the vicinity of the projectiles. The mutual interaction of two fracture zones starts at t ~ 5 ms, near the full engine deceleration moment. So it is safe to say that we can simplify the problem and to simulate four engines impacts separately without loosing much of accuracy.
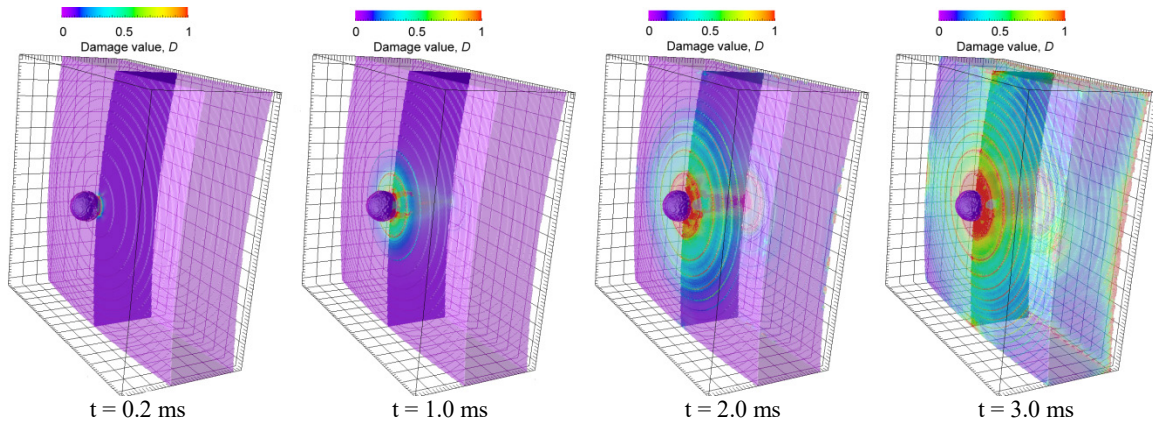

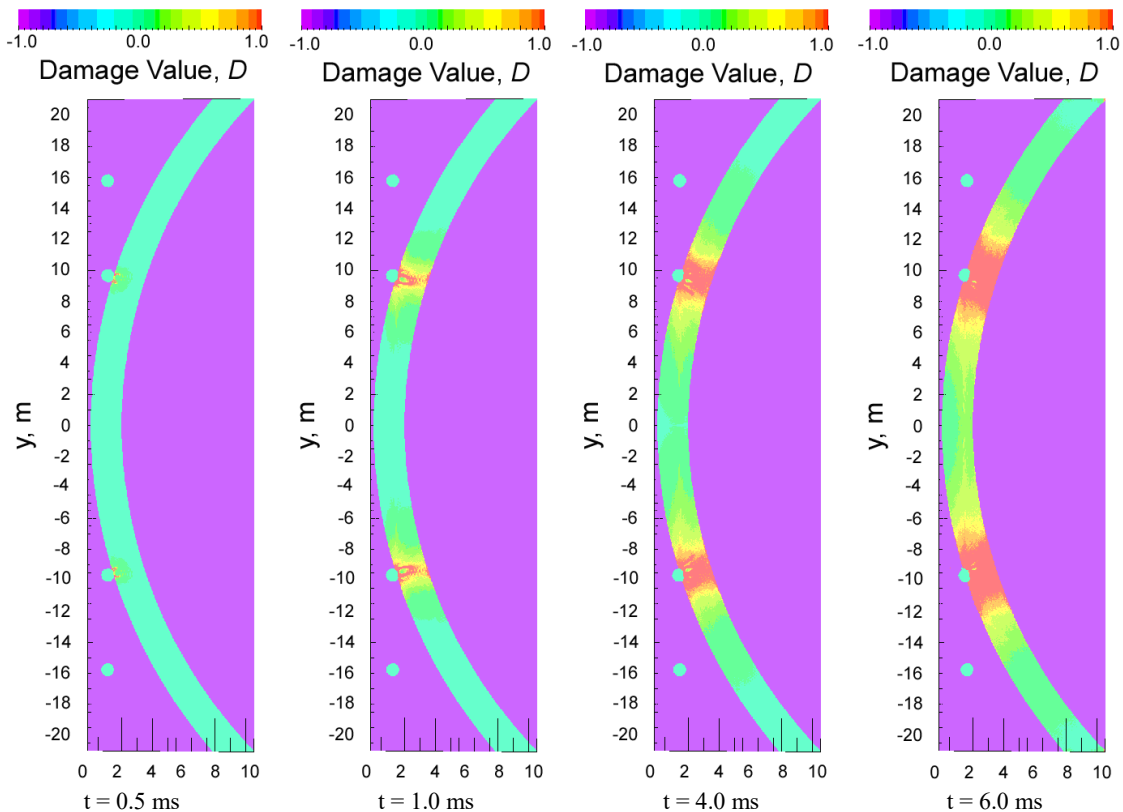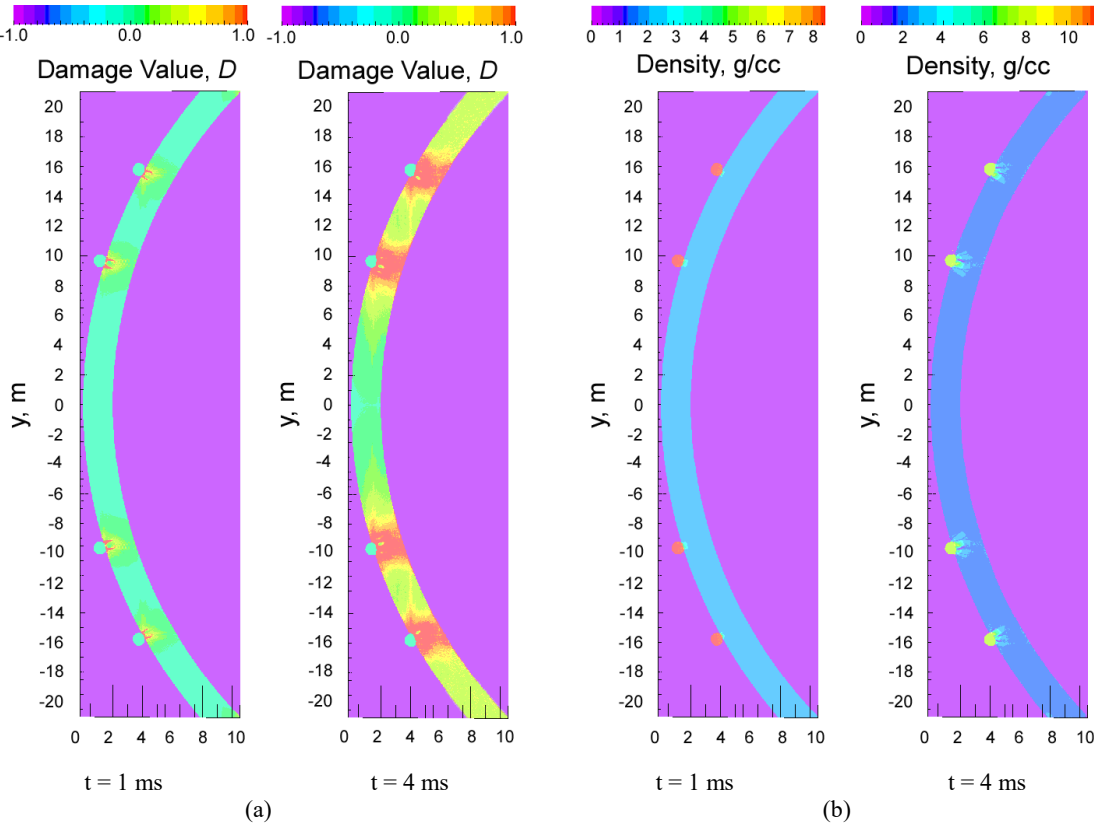FIGURE 4. 3D-distribution of the damage value (D) in the spherical dome

FIGURE 5. 2D-distribution of the damage value (D) in the cylindrical wall of containment during two central engines impact

On the Fig. 6 we present 2D fields of damage value (Fig. 6a) and density (Fig. 6b) distributions for the case of simultaneous impact of all four engines. It also shows that for each engine the fracture and crack formation process goes independently till the later stages of impact (Fig. 6b).

FIGURE 6. 2D-distribution of the damage value (a) and the density (b) in the cylindrical wall of containment during simultaneous four engines impact

CONCLUSION

As a result of this work the system of governing equations for generalization of HJC and Geniev models for non-stationary concrete deformation and fracture was proposed.

The implemented numerical algorithm features high level of numerical stability and is not prone to critical run-time error emergency even in case of total containment destruction.

3D computer modeling showed that containment destruction zones are localized on its free surfaces and near the projectile. With an increase in the impact speed, the braking force becomes higher due to the formation of a compression zone in front of the engine. But the number and depth of the cracks is also increasing. The growth of cracks leads to the formation of a puncture plug when they go to the rear free surface.

Analysis of the results of single- and multiple engines impact simulations showed that the effect of each of the individual engines is localized in the near impact zone and the mutual influence of neighboring impacts at the wave stage of deformation can be neglected. Therefore for BOEING 707-320 aircraft engines impacts can be considered separately. And for the wave stage the cumulative results of an aircraft impact can be simulated by adding up distributions from each of four engines.

ACKNOWLEDGMENTS

REFERENCES

1. M. A. Iqbal et al., Nucl. Eng. Des. **243**, 321 (2012).
2. M. Kostov, F. O. Henkel, and A. Andonov, Nucl. Eng. Des. **269**, 262 (2014).
3. A. Siefert and F. O. Henkel, Nucl. Eng. Des. **269**, 130 (2014).
4. D. K. Thai and S. E. Kim, Nucl. Eng. Des. **293**, 38 (2015).
5. J. D. Riera, Nucl. Eng. Des. **8**(4), 415 (1968).
6. N. A. Chernukha, V. V. Lalin, and A. N. Birbraer, Peter the Great St. Petersburg polytechnic university journal of engineering sciences and technology **23**(04), 159 (2017). In Russian.
7. V. N. Kukudzhanov, Mech. Solids RAS **41**(6), 83 (2006).
8. T. J. Holmquist, G. R. Johnson, and W. H. Cook, "A Computational Constitutive Model for Concrete Subjected to Large Strains, High Strain Rates, and High Pressures," in *Proc. 14th Int. Symp. on Ballistics* (Arlington: ADPA, 1993), p. 794.
9. P. Perzyna and A. Drabik, Arch. Mech. **41(**6), 895 (1989).
10. A. L. Gurson, J. Eng. Mater-T ASME **99**(1), 2 (1977).
11. V. Tvergaard, Int. J. Fracture **17**(4), 389 (1981)
12. C. C. Chu and A. Needleman, J. Eng. Mater-T ASME **102**(3), 249 (1980).
13. V. N. Kukudzhanov, Mech. Solids RAS. **34**(5), 72 (1999). In Russian.
14. M. L. Wilkins, *Calculation of elastic-plastic flow. Methods in Computational Physics* **(**Academic Press, New-York, 1964).
15. V. E. Fortov, V. V. Kim, I. V. Lomonosov, A. V. Matveichev, and A. V. Ostrik, Int. J. Impact Eng. **33**(1-12), 244 (2006).
16. M. W. Evans and F. H. Harlow, LASL Report LA-2139 (1957).
17. A. M. Molodets, A. A. Golyshev, D. V. Shakhray, and V. V. Kim, Phys. Solid State **59**(7), 1406 (2017).
18. N. A. Tahir et al., Physical Review Special Topics - Accelerators and Beams **17**(4), 041003 (2014).
19. V. B. Mintsev et al., Contrib. Plasma Phys. **56(**3-4), 281 (2016).
20. B. A. Klumov, V. V. Kim, I. V. Lomonosov, V. G. Sultanov, A. V. Shutov, and V. E. Fortov, Physics-Uspekhi **48**(7), 733 (2005).
21. V. G. Sultanov, V. V. Kim, I. V. Lomonosov, A. V. Shutov, and V. E. Fortov, Int. J. Impact Eng. **35**(12), 1816 (2008).